JOURNAL OF GUIDANCE, CONTROL, AND DYNAMICS
Vol. 25, No. 6, November–December 2002

Spacecraft Adaptive Attitude and Power Tracking with Variable Speed Control Moment Gyroscopes

Hyungjoo Yoon* and Panagiotis Tsiotras†
Georgia Institute of Technology, Atlanta, Georgia 30332-0150

Control laws for an integrated power/attitude control system (IPACS) for a satellite using variable-speed single-gimbal control moment gyroscopes (VSCMGs) are introduced. Whereas the wheel spin rates of the conventional CMGs are constant, the VSCMGs are allowed to have variable speeds. Therefore, VSCMGs have extra degrees of freedom and can be used to achieve additional objectives, such as energy storage, as well as attitude control. We use VSCMGs in conjunction with an IPACS system. The gimbal rates of the VSCMGs are used to provide the reference-tracking torques, whereas the wheel accelerations are used for both attitude and power reference tracking. The latter objective is achieved by storing or releasing the kinetic energy in the wheels. The control algorithms perform both the attitude and power tracking goals simultaneously. A model-based control and an indirect adaptive control for a spacecraft with uncertain inertia properties are developed. Moreover, control laws for equalization of the wheel speeds are also proposed. Wheel speed equalization distributes evenly the kinetic energy among the wheels, minimizing the possibility of wheel speed saturation and the occurrence of zero-speed singularities. Finally, a numerical example for a satellite in a low Earth, near-polar orbit is provided to test the proposed IPACS algorithm.

Introduction

MOST spacecraft use chemical batteries to store excess energy generated by the solar panels during the period of exposure to the sun. These batteries are used to provide power for the spacecraft subsystems during eclipse and are recharged when the spacecraft is in the sunlight. However, the use of chemical batteries introduces several problems such as limited life cycle, shallow depth of discharge (approximately 20–30% of their rated energy-storage capacity), large weight, and strict temperature limits (at or below 20°C in a low Earth orbit). As a matter of fact, these limitations often drive the entire spacecraft thermal design. Moreover, the use of chemical batteries requires additional system mass for controlling the charging and discharging cycles.

An alternative to chemical batteries is the use of flywheels to store energy. The use of flywheels as "mechanical batteries" has the benefit of increased efficiency (up to 90% depth of discharge with essentially unlimited life) and the ability to operate in a relatively hot (up to 40°C) environment. Most important, flywheels offer the potential to combine the energy-storage and the attitude-control functions into a single device, thus increasing reliability and significantly reducing the overall weight and spacecraft size. This means increased payload capacity and significant reduction of launch and fabrication costs. This concept, termed the integrated power and attitude control system (IPACS) has been studied since the 1960s, but it has become particularly popular during the last decade. The use of flywheels instead of batteries to store energy on spacecraft was suggested as early as 1961 in a paper by Roes,[1] where a 17-W · h/kg composite flywheel spinning at 10,000–20,000 rpm on magnetic bearings was proposed. The configuration included two counter-rotating flywheels, but the author did not mention the possibility of using the momentum stored in the wheels for attitude control. This idea grew over the next three decades. References 2–4 are representative of the period from 1970 to 1977, during which the term IPACS was coined.[2] Reference 5 addresses the optimal bearing control for high-speed momentum wheels (MWs). A complete survey on IPACS is given in Refs. 6 and 7.

To this date, this well-documented IPACS concept has never been implemented on an actual spacecraft mainly because of the high flywheel spin rates required for an efficient IPACS system[8] (on the order of 40,000–80,000 rpm vs less than 6,500 rpm for conventional control moment gyroscopes or momentum wheel actuators). At such high speeds, the actuators quickly wear out traditional mechanical bearings. Additional challenges include flywheel material mass/durability and stiffness inadequacies. Recently, the advances in composite materials and magnetic bearing technology promise to enable a realistic IPACS development. NASA John H. Glenn Research Center at Lewis Field announced that a flywheel energy storage system recently achieved full-speed operation at 60,000 rpm (Ref. 9).

Because flywheels are typically used onboard orbiting satellites to control the attitude, a suitable algorithm must be used to meet simultaneously the attitude torques and the power requirements. In Ref. 6, a control law was presented for an IPACS with momentum wheels. In the present paper a control law for an IPACS using variable-speed single-gimballed control moment gyroscopes (VSCMGs) is introduced. Whereas the wheel spin rates of the conventional CMGs are kept constant, the wheel speeds of the VSCMGs are allowed to vary continuously.[10] Therefore, VSCMGs have extra degrees of freedom and can be used for additional objectives such as energy storage, as well as attitude control. In addition, single-gimbal VSCMGs still have the capability of producing large torques due to their torque amplification property. This makes them ideal for several commercial and military missions. On the other hand, VSCMG motors have to be stronger than standard CMG motors.[10] Because of the higher speeds of the VSCMGs (compared to low-speed momentum of CMG wheels) the power consumption for the VSCMG motors is expected to be several times larger than the one for CMGs. (Standard CMG motors are optimized for low-power consumption at constant speed operation.) Moreover, a significant component of the CMG power consumption, not present in fixed-wheel IPACS, is the power required to provide the gimbal holding torque against the gyroscopic torque along the bearing axis. A comparative study in terms of total power requirements between fixed-wheel CMGs and VSCMGs seems to be desirable in this context.

The VSCMG cluster stores kinetic energy by spinning up its wheels during exposure to the sunlight. It provides power for the

Received 15 October 2001; revision received 29 March 2002; accepted for publication 6 June 2002.

*Graduate Student, School of Aerospace Engineering; hyungjoo_yoon@ae.gatech.edu. Student Member AIAA.

†Associate Professor, School of Aerospace Engineering; p.tsiotras@ae.gatech.edu. Associate Fellow AIAA.

satellite subsystems by despinning the wheels during the eclipse. The spinning-up/spinning-down operation has to be coordinated in such a manner that the generated torques do not disturb the attitude. Most conventional control designs for the IPACS problem use the linearized equations of motion. In this paper, we use the complete, nonlinear equations with minimal assumptions. The derived equations of motion used here for a cluster of VSCMGs are similar to those in Refs. 10 and 11. The only mild assumptions made in deriving these equations are that the spacecraft, flywheels, and gimbal frames are rigid and that the flywheels and gimbals are balanced. In addition, Ref. 10 imposes the assumption that the gimbal frame inertia is negligible. Without loss of generality, in our developments, the gimbal angle rates and reaction wheel accelerations are taken as control inputs to the VSCMG system. That is, as is often done in practice, a velocity steering law is assumed. This implies that the gimbal angle acceleration is kept small. An inner servoloop is used to ensure that the actual gimbal angle rate converges to the desired rate. This is somewhat different than commanding directly gimbal accelerations, that is, acceleration steering law, that typically results in excessive gimbal torque commands.[10,12]

In contrast to previous relevant results,[10,11,13,14] the model-based control presented in this paper achieves tracking of arbitrary trajectories as opposed to only attitude stabilization/regulation. Moreover, the research of Refs. 11 and 14 concentrates on rest-to-rest maneuvers using CMGs with a perfectly known spacecraft model. Although a general trajectory tracking VSCMG control law is presented in Ref. 15, none of the cited references treats the simultaneous attitude and power-tracking problem with VSCMGs.

In addition to the model-based attitude and power-tracking control law presented in this paper, an adaptive control concept is also derived to deal with the uncertainty of the inertia properties of the spacecraft. For exact attitude tracking, the inertia of spacecraft should be known. However, the inertia of spacecraft may change considerably due to docking, releasing a payload, retrieving a satellite, sloshing and/or consumption of fuel, etc., and so an adaptive control scheme is chosen for precise attitude-tracking control. Several adaptive control laws for the attitude-tracking problem have been reported in the literature.[16–22] However, most of the previous results use variable thrust gas jets, momentum or reaction wheels, or conventional CMGs as actuators. An adaptive tracking controller described in Ref. 20 uses Euler angles and Rodriguez parameters (Gibbs vector) to describe the attitude of the spacecraft, so that it is valid only in a narrow range due to the kinematic singularity. In Ref. 18, conventional CMGs are used, and the angular acceleration is required to be measurable. In case the angular acceleration is not measurable, approximation schemes are needed. The adaptive controller developed in Ref. 21 has four asymptotically stable states, one of which is the desired state, and the others are obtained through the rotation by an angle $\pm\pi$ around the axes of the desired frame. These undesired states become unstable if the reference motions are persistently exciting. The adaptive control law in Ref. 16 can be simplified if knowledge of the largest and smallest principal moments of inertia is available. In addition, it is shown that the products of inertia can be identified by constant tracking maneuvers. In Ref. 22, attitude tracking is also dealt with and a controller is proposed which asymptotically approaches the specified response of a linear proportional integral derivative (PID) controller in the presence of inertia errors.

Most mentioned references assume that the unknown inertia parameters are constant, which is not valid for the CMG or VSCMG systems. As far as the authors know, there are no results for adaptive attitude control for a VSCMG system. There have been a few results of adaptive control for a conventional CMG system, but most of them use the linearized or simplified equations of motion.[17,18] Of particular interest is Ref. 19, where adaptation is used to control a double-gimballed CMG with uncertain inertia properties. The present paper offers the first design of an adaptive control using the complete nonlinear equations of motion for a rigid spacecraft with a VSCMG cluster. In addition, this control law achieves both attitude and power tracking.

One of the difficulties encountered with the use of traditional CMGs is the possibility of singularity (gimbal lock) when control torques cannot be generated along certain directions. In addition, conventional momentum wheels have to deal with wheel speed saturation and momentum dumping issues. Control laws for VSCMGs must address both the CMG singularity as well as the momentum wheel saturation problem. Moreover, because the VSCMGs are used as energy storage devices, it is important that none of the VSCMGs despins completely. To keep this from happening, an algorithm to equalize the wheel speeds of the VSCMG cluster is proposed. Speed equalization is desirable because it can also reduce the possibility of actuator saturation and/or the occurrence of singular CMG configurations. Two techniques to equalize the wheel speeds are introduced. The merits and pitfalls of each method are discussed in detail. Comparison via numerical examples is provided at the end of the paper.

System Model

Dynamics

Consider a rigid spacecraft with a cluster of N single-gimbal VSCMGs used to provide internal torques. The definition of the axes is shown in Fig. 1. The total angular momentum of a spacecraft with a VSCMG cluster consisting of N wheels can be expressed in the spacecraft body frame as

$$h = J\omega + A_g I_{cg}\dot{\gamma} + A_s I_{ws}\Omega \tag{1}$$

where $\gamma = (\gamma_1, \ldots, \gamma_N)^T \in \mathbb{R}^N$ and $\Omega = (\Omega_1, \ldots, \Omega_N)^T \in \mathbb{R}^N$ are column vectors whose elements are the gimbal angles and the wheel speeds of the VSCMGs with respect to the gimbals, respectively. In Eq. (1) the matrix J is the inertia matrix of the whole spacecraft, defined as

$$J = {}^B I + A_s I_{cs} A_s^T + A_t I_{ct} A_t^T + A_g I_{cg} A_g^T \tag{2}$$

where ${}^B I$ is the combined matrix of inertia of the spacecraft platform and the point masses of the VSCMGs. The matrices $I_{c\star}$ and $I_{w\star}$ are diagonal with elements the values of the inertias of the gimbal plus wheel structure and wheel-only structure of the VSCMGs, respectively. Specifically, $I_{c\star} = I_{g\star} + I_{w\star}$, where $I_{g\star} = \mathrm{diag}[I_{c\star 1}, \ldots, I_{c\star N}]$ and $I_{w\star} = \mathrm{diag}[I_{w\star 1}, \ldots, I_{w\star N}]$, where $\star$ is g, s, or t. The matrices $A_\star \in \mathbb{R}^{3\times N}$ have as columns the gimbal, spin, and transverse directional unit vectors expressed in the body frame. Thus, $A_\star = [e_{\star 1}, \ldots, e_{\star N}]$, where $e_{\star j}$ is the unit column vector for the jth VSCMG along the direction of the gimbal, spin, or transverse axis. Note that $A_s = A_s(\gamma)$ and $A_g = A_g(\gamma)$ and, thus, both matrices A_s and A_g are functions of the gimbal angles. Consequently, the inertia matrix $J = J(\gamma)$ is also a function of the gimbal angles γ, whereas the matrix ${}^B I$ is constant.

The equations of motion are derived by taking the time derivative of the total angular momentum of the system. If h_c is defined as $h_c = A_g I_{cg}\dot{\gamma} + A_s I_{ws}\Omega$, then $h = J\omega + h_c$ and the time derivative of h with respect to the body B frame is

$$\dot{h} = \dot{J}\omega + J\dot{\omega} + \dot{h}_c = -[\omega^\times]h + g_e \tag{3}$$

where g_e is an external torque (assumed here to be zero for simplicity) and, where for any vector $x = (x_1, x_2, x_3)^T \in \mathbb{R}^3$, the notation

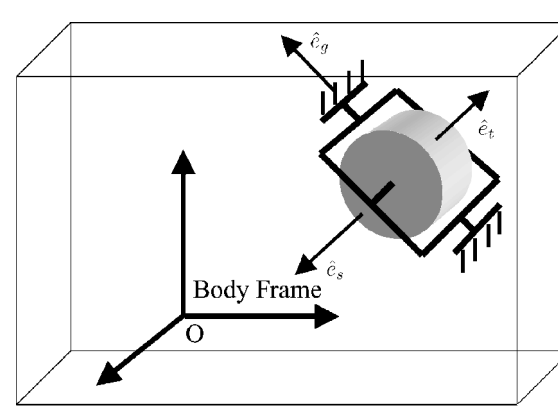

Fig. 1 Spacecraft body with a single VSCMG.

$[x^\times]$ denotes the skew-symmetric matrix

$$[x^\times] = \begin{bmatrix} 0 & -x_3 & x_2 \\ x_3 & 0 & -x_1 \\ -x_2 & x_1 & 0 \end{bmatrix}$$

The matrices A_g, A_s, and A_t can be written using their initial values at time $t = 0$, A_{g0}, A_{s0}, and A_{t0} and the gimbal angles as[14]

$$A_g = A_{g0} \tag{4}$$

$$A_s = A_{s0}[\cos\gamma]^d + A_{t0}[\sin\gamma]^d \tag{5}$$

$$A_t = A_{t0}[\cos\gamma]^d - A_{s0}[\sin\gamma]^d \tag{6}$$

where $\cos\gamma = (\cos\gamma_1, \ldots, \cos\gamma_N)^T \in \mathbb{R}^N$ and $\sin\gamma = (\sin\gamma_1, \ldots, \sin\gamma_N)^T \in \mathbb{R}^N$ and where $[x]^d \in \mathbb{R}^{N\times N}$ is a diagonal matrix with its elements the components of the vector $x \in \mathbb{R}^N$,

$$[x]^d = \begin{bmatrix} x_1 & 0 & \cdots & 0 \\ 0 & x_2 & \cdots & \vdots \\ \vdots & \vdots & \ddots & \vdots \\ 0 & \cdots & \cdots & x_N \end{bmatrix}$$

When Eqs. (4–6) are used, a simple calculation shows that $\dot{A}_s = A_t[\dot{\gamma}]^d$ and $\dot{A}_t = -A_s[\dot{\gamma}]^d$. The time derivatives of J and h_c in Eq. (3) are then calculated as

$$\begin{aligned}\dot{h}_c &= A_g I_{cg}\ddot{\gamma} + \dot{A}_s I_{ws}\Omega + A_s I_{ws}\dot{\Omega} \\ &= A_g I_{cg}\ddot{\gamma} + A_t I_{ws}[\Omega]^d\dot{\gamma} + A_s I_{ws}\dot{\Omega}\end{aligned} \tag{7}$$

$$\dot{J} = A_t[\dot{\gamma}]^d(I_{cs} - I_{ct})A_s^T + A_s[\dot{\gamma}]^d(I_{cs} - I_{ct})A_t^T \tag{8}$$

where we have made use of the obvious fact that $[\dot{\gamma}]^d\Omega = [\Omega]^d\dot{\gamma}$. Finally, the dynamic equations take the form

$$\begin{aligned}&\left\{A_t[\dot{\gamma}]^d(I_{cs} - I_{ct})A_s^T + A_s[\dot{\gamma}]^d(I_{cs} - I_{ct})A_t^T\right\}\omega \\ &\quad + J\dot{\omega} + A_g I_{cg}\ddot{\gamma} + A_t I_{ws}[\Omega]^d\dot{\gamma} + A_s I_{ws}\dot{\Omega} \\ &\quad + [\omega^\times](J\omega + A_g I_{cg}\dot{\gamma} + A_s I_{ws}\Omega) = 0\end{aligned} \tag{9}$$

Note that the equations for a VSCMG system can also be applied to a reaction/momemtum wheel system by letting the gimbal angles γ be constant. They can also be applied to a conventional CMG system by letting the wheel rotation speeds Ω be constant.

Kinematics

The so-called modified Rodrigues parameters (MRPs) given in Refs. 23–25 are chosen to describe the attitude kinematics error of the spacecraft. The MRPs are defined in terms of the Euler principal unit vector $\hat{\eta}$ and angle ϕ by

$$\sigma = \hat{\eta}\tan(\phi/4)$$

The MRPs have the advantage of being well defined for the whole range for rotations,[23,24,26] that is, $\phi \in [0, 2\pi)$. The differential equation that governs the kinematics in terms of the MRPs is given by

$$\dot{\sigma} = G(\sigma)\omega \tag{10}$$

where

$$G(\sigma) = \tfrac{1}{2}\left\{I + [\sigma^\times] + \sigma\sigma^T - \left[\tfrac{1}{2}(1 + \sigma^T\sigma)\right]I\right\} \tag{11}$$

and I is the 3×3 identity matrix.

We point out that the use of the MRPs to describe the kinematics is done without loss of generality. Any other suitable kinematic description could have been used with the conclusions of the paper remaining essentially the same.

Model-Based Attitude-Tracking Controller

In this section a control law based on Lyapunov stability theory is derived for the attitude-tracking problem. In the sequel, it is assumed that the spacecraft and VSCMGs inertia properties are exactly known.

Lyapunov Stability Condition for Attitude Tracking

Assume that the attitude to be tracked is given in terms of the dynamics and kinematics of a desired reference frame (D frame), that is, in terms of some known functions $\sigma_d(t)$, $\omega_d(t)$, and $\dot{\omega}_d(t)$ for $t \geq 0$. Here, σ_d is the MRP vector presenting the attitude of the D frame with respect to the inertial frame (N frame), and ω_d is the angular velocity of the D frame with respect to the N frame expressed in the B frame. Let ω_d^D be the angular velocity of the D frame expressed in its own frame, and let $\dot{\omega}_d^D$ be the time derivative with respect to the D frame, assumed to be known. Then the following relationships hold:

$$\omega_d = C_D^B\omega_d^D, \qquad \dot{\omega}_d = C_D^B\dot{\omega}_d^D - [\omega^\times]C_D^B\omega_d^D$$

The angular-velocity tracking error written in the body frame (B frame) is defined as $\omega_e = \omega - \omega_d$ and σ_e is the MRP error between the reference frame and the body frame calculated from $C_D^B(\sigma_e) = C_N^B(\sigma)C_D^N(\sigma_d)$. The kinematics of the MRP error is then

$$\dot{\sigma}_e = G(\sigma_e)\omega_e$$

A feedback control law to render $\omega_e \to 0$ and $\sigma_e \to 0$ is found using the Lyapunov function[6,10,23]

$$V = \tfrac{1}{2}\omega_e^T J\omega_e + 2k_0\ln\left(1 + \sigma_e^T\sigma_e\right) \tag{12}$$

where $k_0 > 0$. This function is positive definite and radially unbounded in terms of the tracking errors ω_e and σ_e. The time derivative of V is

$$\begin{aligned}\dot{V} &= \frac{1}{2}(\omega - \omega_d)^T\dot{J}(\omega - \omega_d) + (\omega - \omega_d)^T J(\dot{\omega} - \dot{\omega}_d) \\ &\quad + 2k_0\frac{2\sigma_e^T\dot{\sigma}_e}{1 + \sigma_e^T\sigma_e} = -(\omega - \omega_d)^T \\ &\quad \times \left\{-\frac{1}{2}\dot{J}(\omega - \omega_d) - J(\dot{\omega} - \dot{\omega}_d) - k_0\sigma_e\right\}\end{aligned}$$

The preceding equation suggests that, for Lyapunov stability, the choice

$$-\tfrac{1}{2}\dot{J}(\omega - \omega_d) - J(\dot{\omega} - \dot{\omega}_d) - k_0\sigma_e = K_1(\omega - \omega_d) \tag{13}$$

where K_1 is a 3×3 positive definite matrix results in global asymptotic stability of the closed-loop system. [Strictly speaking, the choice of Eq. (13) proves only Lyapunov stability. Asymptotic convergence to the origin follows from a straightforward argument using La Salle's invariant set theory; see, for instance, Refs. 6 and 27. For the sake of brevity, we omit the details of the proof.] Equation (3) then implies that

$$\begin{aligned}&\dot{h}_c + \tfrac{1}{2}\dot{J}(\omega + \omega_d) + [\omega^\times]A_g I_{cg}\dot{\gamma} = K_1(\omega - \omega_d) \\ &\quad + k_0\sigma_e - J\dot{\omega}_d - [\omega^\times](J\omega + A_s I_{ws}\Omega)\end{aligned} \tag{14}$$

The left-hand side (LHS) of Eq. (14) contains the control inputs $\dot{\gamma}$ and $\dot{\Omega}$. In particular, it can be shown that

$$\dot{h}_c + \tfrac{1}{2}\dot{J}(\omega + \omega_d) + [\omega^\times]A_g I_{cg}\dot{\gamma} = B\ddot{\gamma} + C\dot{\gamma} + D\dot{\Omega} = L_{rm}$$

where

$$B = A_g I_{cg} \tag{15}$$

$$\begin{aligned}C = A_t I_{ws}[\Omega]^d + [\omega^\times]A_g I_{cg} + \tfrac{1}{2}\Big[&\left(e_{s1}e_{t1}^T + e_{t1}e_{s1}^T\right)(\omega + \omega_d), \ldots, \\ &\left(e_{sN}e_{tN}^T + e_{tN}e_{sN}^T\right)(\omega + \omega_d)\Big](I_{cs} - I_{ct})\end{aligned} \tag{16}$$

$$D = A_s I_{ws} \tag{17}$$

When the right-hand side (RHS) of Eq. (14) is denoted as the required control torque L_{rm} for attitude tracking

$$L_{rm} = K_1(\omega - \omega_d) + k_0\sigma_e - J\dot{\omega}_d - [\omega^\times](J\omega + A_s I_{ws}\Omega)$$

one obtains that the control inputs must be chosen as

$$B\ddot{\gamma} + C\dot{\gamma} + D\dot{\Omega} = L_{rm} \tag{18}$$

Velocity-Based Steering Law for Attitude Tracking

Typically, the gimbal acceleration term $B\ddot{\gamma}$ can be ignored because the matrix B is small compared to the matrices C and D (Ref. 10). In this case $\dot{\gamma}$ and $\dot{\Omega}$ can be used as control inputs instead of $\ddot{\gamma}$ and $\dot{\Omega}$. This is referred to in the literature as (gimbal) velocity-based steering law. Let $B\ddot{\gamma} \approx 0$ in Eq. (18); the condition for stabilization then becomes

$$[C \quad D]\begin{bmatrix}\dot{\gamma}\\ \dot{\Omega}\end{bmatrix} = L_{rm} \tag{19}$$

Because I_{ws} and $[\Omega]^d$ are diagonal matrices and the second and third terms in the RHS of Eq. (16) are relatively small, it follows that the column vectors of the C matrix are almost parallel to the transverse axes of the gimbal structure and that the column vectors of the D matrix are parallel to the spin axes of the gimbal structure. Therefore, if there are at least two VSCMGs and their (fixed) gimbal axes are not parallel to each other, and if none of the wheel spin rates becomes zero, the column vectors of C and D always span the three-dimensional space. It follows that this VSCMG system can generate control torques along an arbitrary direction. In other words, such a VSCMG system never falls into the singularity (gimbal lock) of a conventional CMG system because of the extra degrees of freedom provided by the wheel speed control.[10] Moreover, if we have three or more VSCMGs, Eq. (19) is underdetermined, and there exist null-motion solutions that do not have any effect on the generated control torque.[11,13] Therefore, we can use this null motion for power tracking and/or wheel speed equalization. This is discussed in the forthcoming "Power Tracking" section.

Adaptive Attitude Tracking Controller

In this section, we design a control law to deal with the uncertainty associated with the spacecraft inertia matrix. Several research results have been published on adaptive attitude control of spacecraft, but most of these results use gas jets and/or reaction/momentum wheels as actuators. In all of these cases, the spacecraft inertia matrix J is constant. As already stated, a difficulty arises because in the VSCMG (and CMG) case the spacecraft inertia matrix J is not constant because it depends on the gimbal angles γ.

Next, we propose an adaptive control law for the VSCMG case. The approach follows arguments that are similar (but not identical) to standard adaptive control design techniques. In the sequel, we assume that the VSCMG cluster inertia properties are exactly known.

Adaptive Control with VSCMGs

In the VSCMG mode, the inertia matrix J is not constant because it depends on the gimbal angles γ. However, the derivative of J is known because it is determined by the control gimbal commands $\dot{\gamma}$. In this section we use this observation to design an adaptive control law that uses estimates of the elements of J. Although direct adaptive schemes that do not identify the moments of inertia are also possible, knowledge of the inertia matrix is often required to meet other mission objectives. We do not pursue such direct adaptive schemes in this work. Of course, as with all typical adaptive control schemes, persistency of excitation of the trajectory is required to identify the correct values of the inertia matrix. Nonetheless, in all cases it is shown that the controller stabilizes the system.

First, we rewrite the equations of the system (9) as

$$\tfrac{1}{2}\dot{J}\omega + J\dot{\omega} + [\omega^\times](J\omega + A_s I_{ws}\Omega) + B\ddot{\gamma} + \tilde{C}\dot{\gamma} + D\dot{\Omega} = 0 \tag{20}$$

where B and D as in Eqs. (15) and (17) and where

$$\tilde{C} = A_t I_{ws}[\Omega]^d + [\omega^\times]A_g I_{cg} + \tfrac{1}{2}\Big[\big(e_{s1}e_{t1}^T + e_{t1}e_{s1}^T\big)\omega, \ldots, (e_{sN}e_{tN}^T + e_{tN}e_{sN}^T)\omega\Big](I_{cs} - I_{ct}) \tag{21}$$

We again make the assumption that the term $B\ddot{\gamma}$ can be neglected, and hence, the system dynamics reduce to

$$\tfrac{1}{2}\dot{J}\omega + J\dot{\omega} + [\omega^\times](J\omega + A_s I_{ws}\Omega) + \tilde{C}\dot{\gamma} + D\dot{\Omega} = 0 \tag{22}$$

By differentiating now Eq. (10), one obtains

$$\omega = G^{-1}(\sigma)\dot{\sigma}, \qquad \ddot{\sigma} = G(\sigma)\dot{\omega} + \dot{G}(\sigma,\dot{\sigma})\omega$$

and by use of Eq. (22),

$$JG^{-1}(\sigma)\ddot{\sigma} = JG^{-1}(\sigma)\dot{G}(\sigma,\dot{\sigma})\omega + J\dot{\omega} = JG^{-1}(\sigma)\dot{G}(\sigma,\dot{\sigma})\omega - [\omega^\times](J\omega + A_s I_{ws}\Omega) - \tilde{C}\dot{\gamma} - D\dot{\Omega} - \tfrac{1}{2}\dot{J}\omega$$

Let $h_1 = J\omega$ and $h_2 = A_s I_{ws}\Omega$. The equation of the system can then be written in standard form:

$$H^*(\sigma)\ddot{\sigma} + C^*(\sigma,\dot{\sigma})\dot{\sigma} = F \tag{23}$$

where

$$H^*(\sigma) = G^{-T}(\sigma)JG^{-1}(\sigma)$$

$$C^*(\sigma,\dot{\sigma}) = -G^{-T}(\sigma)JG^{-1}(\sigma)\dot{G}(\sigma,\dot{\sigma})G^{-1}(\sigma) - G^{-T}(\sigma)\big[h_1^\times\big]G^{-1}(\sigma)$$

$$F = G^{-T}(\sigma)\big[h_2^\times\big]\omega - G^{-T}(\sigma)(\tilde{C}\dot{\gamma} + D\dot{\Omega}) - \tfrac{1}{2}G^{-T}(\sigma)\dot{J}\omega$$

Note that the LHS of Eq. (23) is linear in terms of the elements of J, which are the unknown parameters to be estimated.

The term $\dot{G}(\sigma,\dot{\sigma})$ can be derived by differentiating Eq. (11) as

$$\dot{G}(\sigma,\dot{\sigma}) = \tfrac{1}{2}([\dot{\sigma}^\times] + \dot{\sigma}\sigma^T + \sigma\dot{\sigma}^T - \dot{\sigma}^T\sigma I) \tag{24}$$

Using the fact that $\mathrm{d}/\mathrm{d}t\,(G^{-1}) = -G^{-1}\dot{G}G^{-1}$, we have

$$\dot{H}^* - 2C^* = \frac{\mathrm{d}}{\mathrm{d}t}(G^{-T})JG^{-1} - G^{-T}J\frac{\mathrm{d}}{\mathrm{d}t}(G^{-1}) + 2G^{-T}\big[h_1^\times\big]G^{-1} + G^{-T}(\sigma)\dot{J}G^{-1}(\sigma)$$

which implies that the matrix $(\dot{H}^* - 2C^* - G^{-T}\dot{J}G^{-1})$ is skew symmetric.

The remaining procedure follows one of the standard adaptive control design methods.[20] To this end, let $a \in \mathbb{R}^6$ be the parameter vector defined by

$$a = (J_{11}, J_{12}, J_{13}, J_{22}, J_{23}, J_{33})^T \tag{25}$$

and let $\hat{a}$ be the parameter vector estimate. The parameter estimation error is $\tilde{a} = \hat{a} - a$, and $\tilde{\sigma} = \sigma - \sigma_d$ is the attitude tracking error. Consider now the Lyapunov-like function

$$V_a = \tfrac{1}{2}s^T H^*(\sigma)s + \tfrac{1}{2}\tilde{a}^T\Gamma^{-1}\tilde{a} \tag{26}$$

where Γ is a strictly positive constant matrix and $s = \dot{\tilde{\sigma}} + \lambda\tilde{\sigma} = \dot{\sigma} - \dot{\sigma}_r$ $(\lambda > 0)$ is a measure of the attitude tracking error. Note that $\dot{\sigma}_r = \dot{\sigma}_d - \lambda\tilde{\sigma}$ is the reference velocity vector. Differentiating V_a, and using the skew-symmetry of the matrix $(\dot{H}^* - 2C^* - G^{-T}\dot{J}G^{-1})$, one obtains

$$\dot{V}_a = s^T\big[F - H^*(\sigma)\ddot{\sigma}_r - C^*(\sigma,\dot{\sigma})\dot{\sigma}_r + \tfrac{1}{2}G^{-T}(\sigma)\dot{J}G^{-1}(\sigma)s\big] + \tilde{a}^T\Gamma^{-1}\dot{\tilde{a}}$$

Let a control law be such that

$$F = \hat{H}^*(\sigma)\ddot{\sigma}_r + \hat{C}^*(\sigma,\dot{\sigma})\dot{\sigma}_r - K_D s - \tfrac{1}{2}G^{-T}(\sigma)\dot{J}G^{-1}(\sigma)s \tag{27}$$

where $\hat{H}^* = G^{-T}\hat{J}G^{-1}$ and $\hat{C}^* = -G^{-T}\hat{J}G^{-1}\dot{G}G^{-1} - G^{-T}[\hat{h}_1^\times]G^{-1}$ and where K_D is a symmetric positive definite matrix. Then it follows that

$$\dot{V}_a = s^T\left[\tilde{H}^*(\sigma)\ddot{\sigma}_r + \tilde{C}^*(\sigma,\dot{\sigma})\dot{\sigma}_r - K_D s\right] + \tilde{a}^T\Gamma^{-1}(\dot{\hat{a}} - \dot{a})$$

where $\tilde{H}^*(\sigma) = \hat{H}^*(\sigma) - H^*(\sigma)$ and $\tilde{C}^*(\sigma,\dot{\sigma}) = \hat{C}^*(\sigma,\dot{\sigma}) - C^*(\sigma,\dot{\sigma})$. Note that Eq. (8) implies that $\dot{a}$ is known if $\dot{\gamma}$ is known.

The linear parameterization of the dynamics allows us to define a known matrix $Y^*(\sigma,\dot{\sigma},\dot{\sigma}_r,\ddot{\sigma}_r)$ such that

$$\tilde{H}^*(\sigma)\ddot{\sigma}_r + \tilde{C}^*(\sigma,\dot{\sigma})\dot{\sigma}_r = Y^*(\sigma,\dot{\sigma},\dot{\sigma}_r,\ddot{\sigma}_r)\tilde{a} \tag{28}$$

Choosing the adaptation law as

$$\dot{\hat{a}} = -\Gamma(Y^*)^T s + \dot{a} \tag{29}$$

yields $\dot{V}_a = -s^T K_D s \le 0$. The last inequality implies boundedness of s and $\tilde{a}$ and, in addition, that $s \to 0$. Using standard arguments,[20,27] it follows that $\sigma \to \sigma_d$. Therefore, global asymptotic stability of the attitude-tracking error is guaranteed.

From Eq. (27) it follows that the required control inputs are obtained by solving

$$[C \quad D]\begin{bmatrix}\dot{\gamma}\\ \dot{\Omega}\end{bmatrix} = L_{ra} \tag{30}$$

where $D = A_s I_{ws}$ and

$$C = A_t I_{ws}[\Omega]^d + [\omega^\times]A_g I_{cg} + \tfrac{1}{2}\left[\left(e_{s1}e_{t1}^T + e_{t1}e_{s1}^T\right)\left(\omega + G^{-1}\dot{\sigma}_r\right), \ldots, \left(e_{sN}e_{tN}^T + e_{tN}e_{sN}^T\right)\left(\omega + G^{-1}\dot{\sigma}_r\right)\right](I_{cs} - I_{ct}) \tag{31}$$

and where

$$L_{ra} = -G^T(\sigma)\left[\hat{H}^*(\sigma)\ddot{\sigma}_r + \hat{C}^*\dot{\sigma}_r - K_D s\right] + \left[h_2^\times\right]\omega \tag{32}$$

Once $\dot{\gamma}$ is known from the solution of Eq. (30), it can be substituted in the adaptive control law in Eq. (29).

Remark: Usually the combined matrix of inertia of the spacecraft platform and the point masses of VSCMGs, ${}^B I$, occupies most of the total matrix of inertia $J(\gamma)$, and the γ-dependent part of the inertia matrix is relatively small. In such a case, we can assume that J is a constant matrix. With this assumption, the equation of the system (20) can be written in a simplified form as

$$J\dot{\omega} + [\omega^\times](J\omega + A_s I_{ws}\Omega) + B\ddot{\gamma} + \tilde{C}_s\dot{\gamma} + D\dot{\Omega} = 0 \tag{33}$$

where B and D are as in Eqs. (15) and (17) and where $\tilde{C}_s = A_t I_{ws}[\Omega]^d + [\omega^\times]A_g I_{cg}$. The equation in the standard form [Eq. (23)] remains the same, except that now F becomes

$$F_s = G^{-T}(\sigma)\left[h_2^\times\right]\omega - G^{-T}(\sigma)(\tilde{C}_s\dot{\gamma} + D\dot{\Omega})$$

Moreover, we have

$$\dot{H}^* - 2C^* = \frac{\mathrm{d}}{\mathrm{d}t}(G^{-T})JG^{-1} - G^{-T}J\frac{\mathrm{d}}{\mathrm{d}t}(G^{-1}) + 2G^{-T}\left[h_1^\times\right]G^{-1}$$

which implies that the matrix $\dot{H}^* - 2C^*$ is skew symmetric. Therefore, the required control input is obtained by solving Eq. (30) with $\tilde{C}_s$ instead of C. The adaptation law also simplifies to

$$\dot{\hat{a}} = -\Gamma(Y^*)^T s \tag{34}$$

Acceleration-Based Steering Law for Attitude Tracking

The gimbal motors require angle acceleration (equivalently, torque) commands instead of gimbal rate commands. The control law in terms of $\dot{\gamma}$ has then to be implemented via another feedback loop around the gimbal angle acceleration. For instance, once the reference or desired gimbal rate command $\dot{\gamma}_d$ has been determined from, for example, Eq. (19) or Eq. (30), the gimbal acceleration (and, hence, torque) command can be computed from

$$\ddot{\gamma} = K_4(\dot{\gamma} - \dot{\gamma}_d) + \ddot{\gamma}_d \approx K_4(\dot{\gamma} - \dot{\gamma}_d) \tag{35}$$

where K_4 is a 4×4 matrix of controller gains. When the matrix K_4 is chosen to be Hurwitz, this control law will force the actual gimbal rates $\dot{\gamma}$ to track $\dot{\gamma}_d$ as $t \to \infty$.

Power Tracking

In Ref. 6 a solution to the simultaneous attitude and power-tracking problem was given for the case of a rigid spacecraft with N momentum wheels. In this section, we extend these results to the case of N VSCMGs. By setting the gimbal angles to a constant value, we can retrieve the results of Ref. 6 as a special case.

The total (useful) kinetic energy stored in the momentum wheels is

$$T = \tfrac{1}{2}\Omega^T I_{ws}\Omega$$

Hence, the power (rate of change of the energy) is given by

$$P = \frac{\mathrm{d}T}{\mathrm{d}t} = \Omega^T I_{ws}\dot{\Omega} = \begin{bmatrix}0 & \Omega^T I_{ws}\end{bmatrix}\begin{bmatrix}\dot{\gamma}\\ \dot{\Omega}\end{bmatrix} \tag{36}$$

This equation is augmented to the attitude-tracking equation (19) or Eq. (30), to obtain the equation for IPACS with VSCMG as follows:

$$Qu = L_{rp} \tag{37}$$

where

$$u = \begin{bmatrix}\dot{\gamma}\\ \dot{\Omega}\end{bmatrix}, \qquad Q_{4\times 2N} = \begin{bmatrix}C_{3\times N} & D_{3\times N}\\ 0_{1\times N} & \left(\Omega^T I_{ws}\right)_{1\times N}\end{bmatrix}$$

$$L_{rp} = \begin{bmatrix}L_r\\ P\end{bmatrix} \tag{38}$$

and P is the required power and L_r is either L_{rm} or L_{ra}, depending on the attitude controller used.

Solution of Velocity Steering Law for IPACS

If the Q matrix has rank 4 (is full row rank), Eq. (37) has infinitely many solutions and the minimum-norm solution, which is generally chosen among the solutions to reduce the input, can be calculated from

$$u = Q^T(QQ^T)^{-1}L_{rp} \tag{39}$$

If the C matrix in Eq. (38) has rank 3 (is full row rank), then the matrix Q is also full row rank, and the control can be calculated from Eq. (39). If, however, the C matrix has rank 2, then Q may be rank deficient, and an exact solution that satisfies Eq. (37) does not exist unless L_{rp} is in the range of Q. Otherwise, only an approximate solution can be calculated from $u = Q^\dagger L_{rp}$, where $Q^\dagger$ is the Moore–Penrose inverse of Q. [Because the Moore–Penrose inverse solution becomes equal to Eq. (39) when Q is full row rank, we can always choose this solution regardless of the rank of Q.] In this case, simultaneous attitude and power tracking is not possible, except in very special cases.[6]

Although the rank deficiency of the C matrix can be reduced using more VSCMGs, the possibility of a singularity still remains. Moreover, if the minimum-norm solution of Eq. (37) is used for control, this solution tends to steer the gimbals toward the rank deficiency states.[28–30] This happens because the projection of the generated torques along the required torque direction is maximum when the transverse axis of the gimbal (the axis along which torque can be generated in CMG mode) is close to the required torque. Thus, the minimum-norm solution tends to use the gimbals whose configuration is far from the rank deficiency states. Several methods have been proposed for keeping the matrix C full rank using null motion.[10,11,13,30] In particular, Schaub et al.[10] suggested a singularity avoidance method using a VSCMG system.

It is advantageous for the VSCMGs to act as conventional CMGs to make the most out of the torque amplification effect, which is the most significant merit of the CMGs. A weighted minimum-norm solution, which minimizes the weighted cost

$$\mathcal{J}_2 = \tfrac{1}{2}u^T W^{-1}u \tag{40}$$

can be used to operate between the CMG and MW modes.[10] For example, if the weighting matrix W is defined as

$$W = \begin{bmatrix} w_1 e^{-w_2 \sigma_c} I_N & 0_N \\ 0_N & I_N \end{bmatrix} \tag{41}$$

where I_N is the $N \times N$ identity matrix and where σ_c is the condition number of C (the ratio of the largest to the smallest singular value) and w_1 and w_2 are positive gains chosen by the user, the weighted minimum-norm solution control law is given by

$$u = WQ^T(QWQ^T)^{-1}L_{rp} \tag{42}$$

In case Q is not full row rank, the approximate solution can be obtained from

$$u = W^{\frac{1}{2}}\left(QW^{\frac{1}{2}}\right)^{\dagger}L_{rp} \tag{43}$$

Note that according to the condition number of the matrix C, the VSCMG can operate either as a MW (close to a CMG singularity, i.e., when σ_c is large) or as a regular CMG (away from a singularity, i.e., when σ_c is small). As a CMG singularity is approached, the VSCMGs will smoothly switch to a momentum wheel mode. As a result, this method can also handle temporary rank deficiencies of the matrix C (Ref. 10). In this work, the condition number of the matrix C is used as a measure of closeness of the matrix C to being rank deficient. Larger condition numbers mean a more "singular" matrix C. This is a more reliable measure of rank deficiency of a matrix than, for example, the determinant of the matrix.[31] The condition numbers have also been used in Refs. 11 and 13.

Notice that a purely MW mode can be enforced by letting W in Eq. (42) be

$$W_{\mathrm{MW}} = \begin{bmatrix} 0_N & 0_N \\ 0_N & I_N \end{bmatrix}$$

A conventional CMG operation is enforced if W in Eq. (42) is chosen as

$$W_{\mathrm{CMG}} = \begin{bmatrix} I_N & 0_N \\ 0_N & 0_N \end{bmatrix}$$

As alluded to in the Introduction, in MW mode the VSCMGs are power inefficient (when compared to low-speed flywheels). Under normal conditions, however, the MW mode will be engaged only sporadically, and for short periods of time, to provide the necessary torque (albeit in a power-inefficient manner) near singularities.

Wheel Speed Equalization

If some of the wheel spin rates become too small, a change of the gimbal angle cannot generate the required torque. If this is the case, the remaining degrees of freedom may not be enough to allow exact attitude and power tracking. On the other hand, if some of the wheel spin rates become too high, some of the wheels may saturate. Desaturation of the wheels requires thruster firing, thus depleting valuable fuel. To minimize the possibility of singularity and/or wheel saturation, it is desirable to equalize the wheel spinning rates of the VSCMGs, whenever possible. Next, we propose two control laws to achieve wheel speed equalization for a VSCMG-based IPACS.

The first method adds an extra constraint that forces the wheel speeds to converge to the average wheel speed of the cluster. By the introduction of

$$\mathcal{J}_{w1}(\Omega_1, \ldots, \Omega_N) = \frac{1}{2}\sum_{i=1}^{N}(\Omega_i - \bar{\Omega})^2 = \frac{1}{2}\Omega_e^T\Omega_e \tag{44}$$

where

$$\bar{\Omega} = \frac{1}{N}\sum_{i=1}^{N}\Omega_i, \qquad \Omega_e = \Omega - \bar{\Omega}\mathbf{1}_{N\times 1}$$

and $\mathbf{1}_{N\times 1}$ is $N \times 1$ vector whose elements are 1s, the condition for equalization is expressed as the requirement that

$$\frac{\mathrm{d}}{\mathrm{d}t}\mathcal{J}_{w1} = \nabla\mathcal{J}_{w1}\dot{\Omega} = \sum_{i=1}^{N}\frac{\partial\mathcal{J}_{w1}}{\partial\Omega_i}\dot{\Omega}_i = -k_2\mathcal{J}_{w1}$$

where $k_2 > 0$. This condition is augmented in Eq. (37), and the control input u is calculated from this augmented equation. Summarizing, the control law that achieves attitude and power tracking with wheel speed equalization is given by

$$\begin{bmatrix} C & D \\ 0 & \Omega^T I_{ws} \\ 0 & \nabla\mathcal{J}_{w1} \end{bmatrix}\begin{bmatrix} \dot{\gamma} \\ \dot{\Omega} \end{bmatrix} = \begin{bmatrix} L_r \\ P \\ -k_2\mathcal{J}_{w1} \end{bmatrix} \tag{45}$$

and the use of Eq. (42). Using the fact that $\Omega_e = [I_N - (1/N)\mathbf{1}_{N\times N}]\Omega$, where $\mathbf{1}_{N\times N}$ is $N \times N$ matrix whose elements are 1s, and the fact that the matrix $[I_N - (1/N)\mathbf{1}_{N\times N}]$ is idempotent, it can be easily shown that $\nabla\mathcal{J}_{w1} = \Omega_e^T$. (Note that a matrix A is idempotent if $A^2 = A$.)

The second method uses a modified cost of Eq. (40) in which the directions of wheel speed changes are considered. The cost to be minimized in this case is expressed as

$$\mathcal{J}_{w2} = \tfrac{1}{2}u^T W^{-1}u + Ru \tag{46}$$

The weighting matrix R is determined so that the wheels that rotate faster or slower than the average wheel speed are suitably penalized. For instance, one may choose

$$R = \begin{bmatrix} 0_{1\times N} & k_3\Omega_e^T \end{bmatrix} \tag{47}$$

where $k_3 > 0$. The motivation for this choice for R stems from the following observation. Notice that with R as in Eq. (47) we have

$$Ru = \sum_{i=1}^{N}(\Omega_i - \bar{\Omega})\dot{\Omega}_i$$

If $\Omega_i > \bar{\Omega}$ for some i, then Ru is minimized by choosing $\dot{\Omega}_i < 0$, that is, by making Ω_i tend closer to $\bar{\Omega}$. If, on the other hand, $\Omega_i < \bar{\Omega}$, then Ru is minimized by choosing $\dot{\Omega}_i > 0$, forcing again Ω_i toward $\bar{\Omega}$. Of course, the linear term Ru does not have an unconstrained minimum; hence, a quadratic term is included in Eq. (46) to ensure that the minimization problem has a solution.

The solution that minimizes the cost (46) subject to the equality constraint (37) is

$$u = W\left[Q^T(QWQ^T)^{-1}\left(L_{rp} + QWR^T\right) - R^T\right] \tag{48}$$

In case Q is not full row rank, the equation

$$\begin{aligned} u &= W^{\frac{1}{2}}\left(QW^{\frac{1}{2}}\right)^{\dagger}\left(L_{rp} + QWR^T\right) - WR^T \\ &= W^{\frac{1}{2}}\left(QW^{\frac{1}{2}}\right)^{\dagger}L_{rp} - \left[I - W^{\frac{1}{2}}\left(QW^{\frac{1}{2}}\right)^{\dagger}Q\right]WR^T \end{aligned} \tag{49}$$

can be used, instead. Note that this method is identical with the control law without wheel speed equalization if $k_3 = 0$.

It can be shown that with the choice $W = \alpha I$ ($\alpha > 0$), the second method is basically equivalent to so-called the gradient method,[32] which was originally devised for the singularity avoidance problem of conventional CMGs[13,32] using the null motion. The null motion does not have any effect on the generated output torque but has the effect of increasing (or decreasing) the cost function. The null motion of Eq. (37) can be written as

$$\begin{bmatrix} \dot{\gamma} \\ \dot{\Omega} \end{bmatrix}_{\mathrm{null}} = [I - Q^{\dagger}Q]d = \mathcal{P}d, \qquad d \in \mathbb{R}^{2N\times 1} \tag{50}$$

It can be easily shown that $Q[\dot{\gamma}^T, \ \dot{\Omega}^T]^T_{\mathrm{null}} = 0$ and that the projection matrix $\mathcal{P} = [I - Q^{\dagger}Q]$ is idempotent. It is also a symmetric matrix (and, hence, positive semidefinite) because it represents an orthogonal projection onto the null subspace of the matrix Q.

If now the vector d is selected as

$$d = -k_3 \begin{bmatrix} \dfrac{\partial \mathcal{J}_{w1}^T}{\partial \gamma} \\ \dfrac{\partial \mathcal{J}_{w1}^T}{\partial \Omega} \end{bmatrix} \tag{51}$$

then the rate of change of $\mathcal{J}_{w1}$ due to the null motion is

$$\dot{\mathcal{J}}_{w1}|_{\text{null}} = \begin{bmatrix} \dfrac{\partial \mathcal{J}_{w1}}{\partial \gamma} & \dfrac{\partial \mathcal{J}_{w1}}{\partial \Omega} \end{bmatrix} \begin{bmatrix} \dot{\gamma} \\ \dot{\Omega} \end{bmatrix}_{\text{null}}$$

$$= -k_3 \begin{bmatrix} \dfrac{\partial \mathcal{J}_{w1}}{\partial \gamma} & \dfrac{\partial \mathcal{J}_{w1}}{\partial \Omega} \end{bmatrix} \mathcal{P} \begin{bmatrix} \dfrac{\partial \mathcal{J}_{w1}^T}{\partial \gamma} \\ \dfrac{\partial \mathcal{J}_{w1}^T}{\partial \Omega} \end{bmatrix} \leq 0$$

Thus, it is expected that the wheel speeds will be equalized. We also see that in case $W = \alpha I$ the quantity WR^T in Eq. (49) is equal to $-d$ in Eq. (51), because $\partial \mathcal{J}_{w1}/\partial \gamma = 0$ and $\partial \mathcal{J}_{w1}/\partial \Omega = \Omega_e^T$. It follows that the second method is identical to the gradient method.

Each of the preceding two wheel speed equalization algorithms has its own merits and pitfalls. The first one guarantees exact equalization for the IPACS. However, this method uses an additional degree of freedom because one has to solve the augmented linear system (45). The second method, on the other hand, shows a tendency for wheel speed equalization, but it does not guarantee perfect equalization of wheel speeds, in general. The wheel speeds tend to become equal away from the CMG singularity but they exhibit a bifurcation near the singularity because the torques for attitude control must be generated from changes of wheel speeds. However, this method does not use any additional degrees of freedom. If some other objectives such as a singularity avoidance strategy is desired, the second method may be preferable.

Table 1 Simulation parameters

Symbol	Value
N	4
θ	54.75 deg
$\omega(0)$	$[0, 0, 0]^T$ rad/s
$\dot{\omega}(0)$	$[0, 0, 0]^T$ rad/s^2
$\sigma(0)$	$[0, 0, 0]^T$
$\gamma(0)$	$[\pi/2, -\pi/2, -\pi/2, \pi/2]^T$ rad
$\dot{\gamma}(0)$	$[0, 0, 0]^T$ rad/s^2
${}^B I$	$\begin{bmatrix} 15{,}053 & 3{,}000 & -1{,}000 \\ 3{,}000 & 6{,}510 & 2{,}000 \\ -1{,}000 & 2{,}000 & 11{,}122 \end{bmatrix}$ kg · m^2
I_{ws}	diag{0.7, 0.7, 0.7, 0.7} kg · m^2
I_{wt}, I_{wg}	diag{0.4, 0.4, 0.4, 0.4} kg · m^2
I_{gs}, I_{gt}, I_{gg}	diag{0.1, 0.1, 0.1, 0.1} kg · m^2

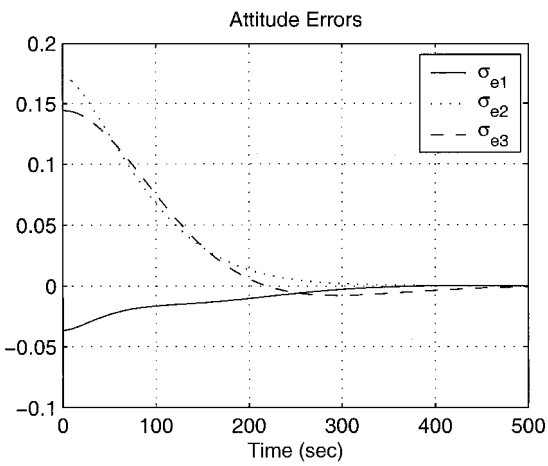

Fig. 2 Attitude error trajectory.

Numerical Examples

A numerical example for a satellite in a low Earth orbit is provided to test the proposed IPACS algorithm. Similar to Refs. 8 and 10, we use a standard four-VSCMG pyramid configuration. In this configuration, the VSCMGs are installed so that the four gimbal axes form a pyramid with respect to the body. The angle of each of the pyramid sides to its base (assumed to be parallel to the spacecraft x–y plane) is given by θ. Table 1 contains the parameters used for the simulations. These parameters closely parallel those used in Refs. 8 and 10.

Two simulation scenarios are presented to demonstrate the validity of the adaptive IPACS and speed equalization control algorithms given in the preceding sections. In the first scenario, a satellite in a

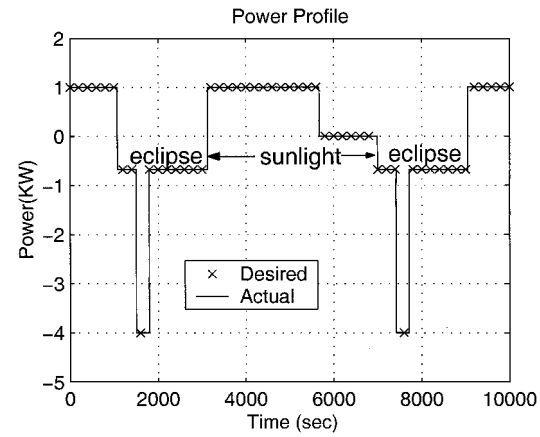

Fig. 3 Desired ×, and actual ——, power profiles.

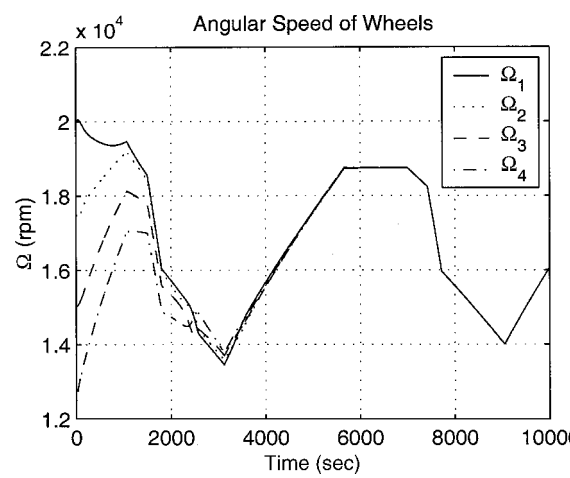

a) Method 1

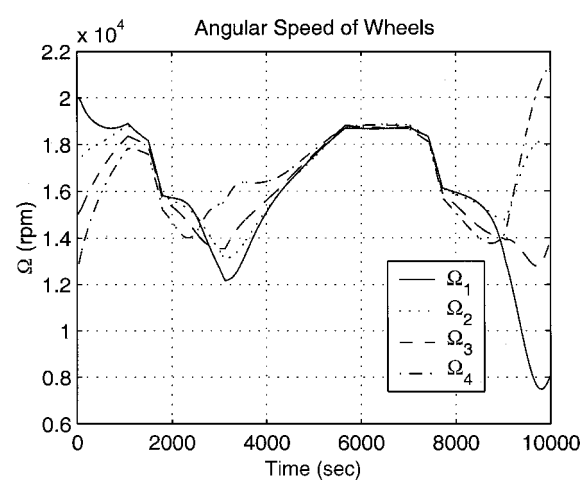

b) Method 2

Fig. 4 Angular wheel speeds with speed equalization.

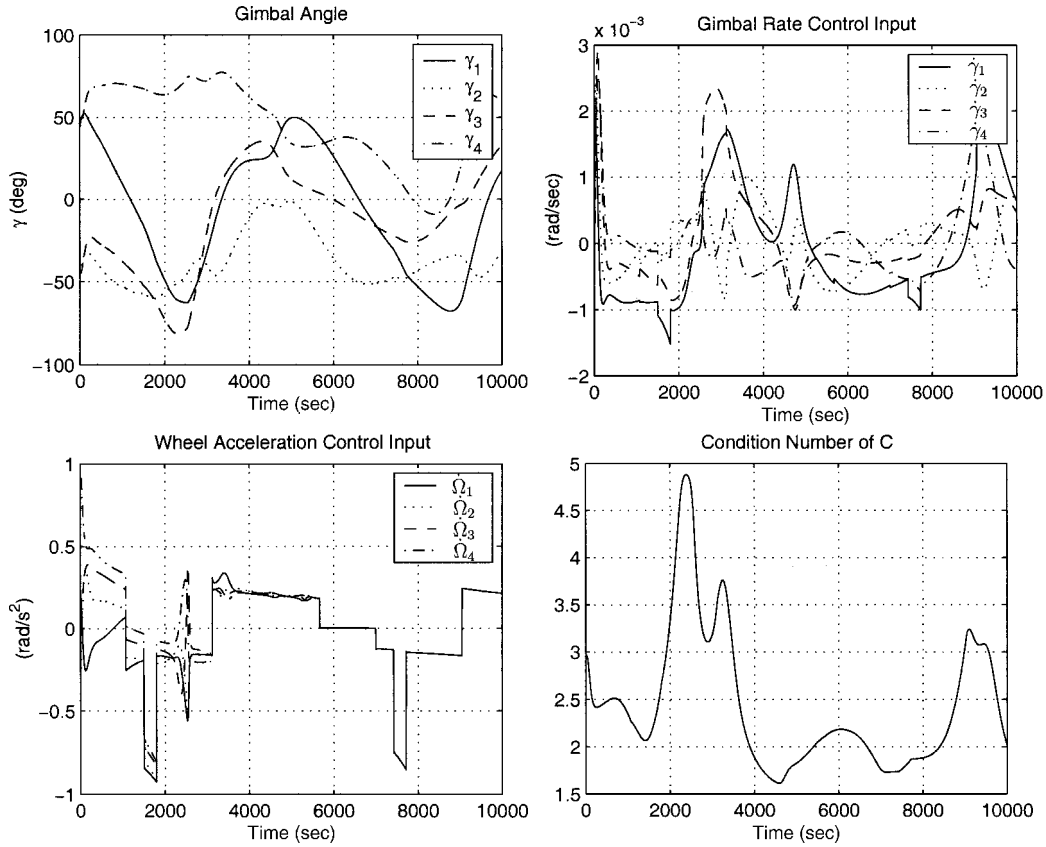

Fig. 5 Gimbal angles, control inputs, and condition number of matrix C (method 1).

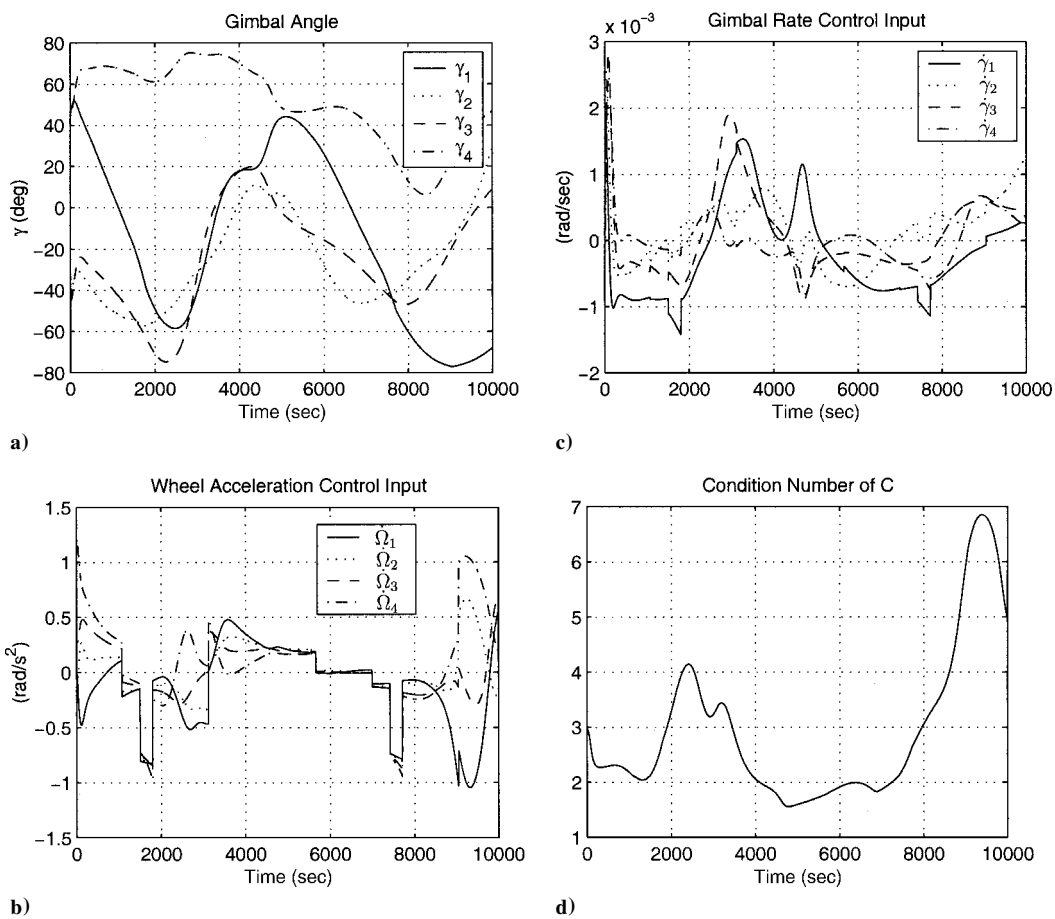

Fig. 6 Gimbal angles, control inputs, and condition number of matrix C (method 2).

near-polar orbit with a period of 98 min is considered. (The orbital data are chosen as in Ref. 6.) The satellite's boresight axis is required to track a ground station, and the satellite is required to rotate about its boresight axis so that the solar panel axis is perpendicular to the satellite–sun axis to maximize the efficiency of the panel. For simplicity, it is assumed that the satellite keeps tracking the ground station and the sun even when these are not directly visible due to the location of the Earth.

During the eclipse (which lasts approximately 35 min), the nominal power requirement is 680 W, with an additional requirement of 4-kW power for 5 min. During sunlight (which lasts approximately 63 min), the wheels are charged with a power level of 1 kW until the total energy stored in the wheels reaches 1.5 kW · h. These attitude- and power-tracking requirements are the same as in Ref. 6. The details of the method used to generated the required attitude, body rate, and body acceleration are also given in the same reference. In this scenario, the spacecraft body frame is initially aligned with the inertial frame. The control gains are chosen as

$$K_D = 4 \times 10^3 I_{3\times 3}, \qquad \Gamma = 1 \times 10^7 I_{6\times 6}, \qquad \lambda = 0.01$$

$$k_2 = 2 \times 10^{-3}, \qquad k_3 = 2 \times 10^{-3}, \qquad K_4 = -2I_{4\times 4}$$

$$w_1 = 1 \times 10^{-4}, \qquad w_2 = 1$$

based on trial and error. As a challenging case, all of the initial parameter estimates are chosen to be zero, which means no initial information about the inertia matrix is available. In practice, any educated estimate of the inertia parameters (or prior experience) can be used to choose the controller gains or the initial parameter estimates accordingly. The results of the numerical simulations are shown next. Figure 2 shows the attitude error. The spacecraft attitude tracks the desired attitude exactly after a short period of time. Figure 3 shows that the actual power profile also tracks the required power command exactly. The crosses indicate the desired power history and the solid line indicates the actual power history. Figures 2 and 3 show that the goal of IPACS is achieved successfully. Figure 4 shows the wheel speed histories when each of the two wheel equalization methods is applied. The corresponding gimbal angles and control signals for both methods are shown in Fig. 5 and 6. The attitude histories are similar for both cases.

As seen from Fig. 4a, the first method achieves exact speed equalization, whereas the second method equalizes the wheels only approximately (Fig. 4b). In fact, after the condition number of the matrix C becomes large (Fig. 6d) the second method switches smoothly to a MW mode, and thus, the wheel speeds deviate from each other. The first method still keeps the wheel speeds equalized after the sudden change of the required power profile, whereas the second method shows a tendency of divergence. As expected, in both cases, the wheels spin-up (charge) during sunlight and despin (discharge) during the eclipse.

Note that in all simulations the moment of inertia matrix has been assumed to be completely unknown. Despite this, the adaptive control law achieves both attitude and power tracking while equalizing the wheel speeds, as desired. Although the control algorithm shows excellent attitude-/power-tracking performance, the reference attitude trajectory in this scenario is too slow to achieve parameter convergence. To emphasize the performance of the adaptive controller, we considered another scenario in which the reference trajectory varies much faster. For illustration purposes, a reference trajectory similar to the coning motion of Ref. 16 is chosen. Initially, the reference attitude is aligned with the actual attitude, and the angular velocity of the reference attitude is chosen as

$$\omega_d(t) = 0.02 \times [\sin(2\pi t/800),\ \sin(2\pi t/600),\ \sin(2\pi t/400)]^T \text{ rad/s}$$

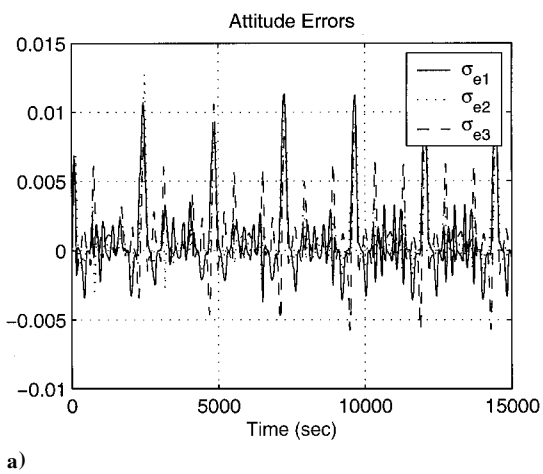

a)

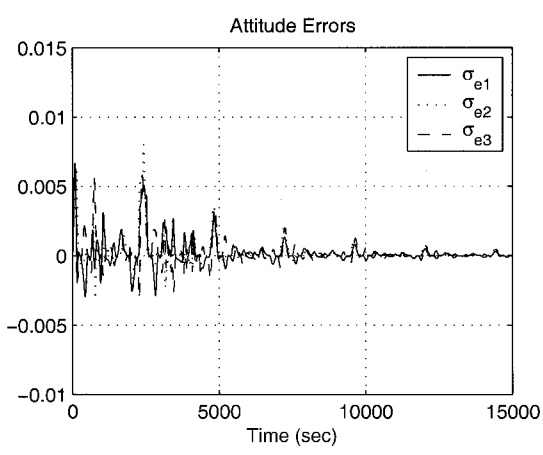

b)

Fig. 7 Attitude error trajectories: a) without adaptation and b) with adaptation.

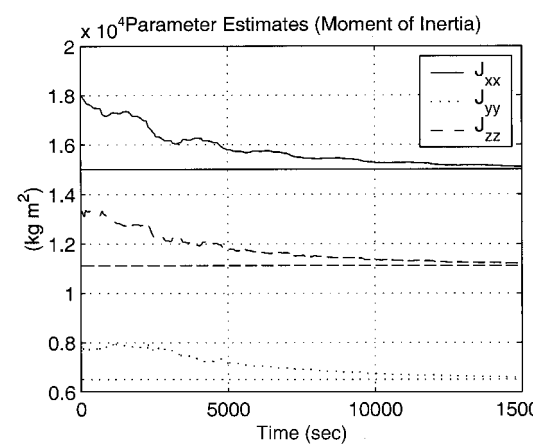

J_{xx}, J_{yy}, J_{zz}

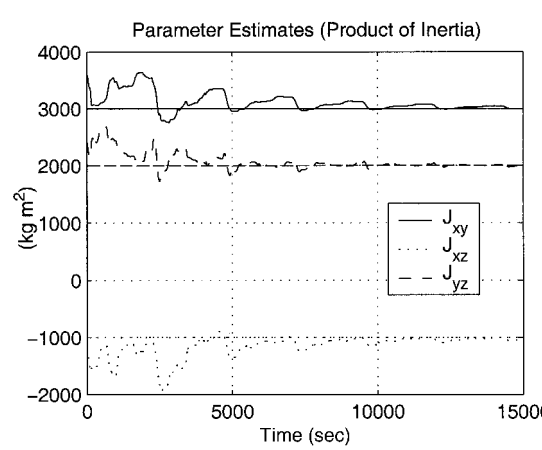

J_{xy}, J_{xz}, J_{yz}

Fig. 8 Parameter convergence for coning motion.

A 20% uncertainty in the spacecraft nominal inertia matrix ${}^{B}I$ is assumed. Figure 7 shows the attitude error trajectories with and without adaptation. These simulation results show that the designed adaptive control gives significantly improved performance over the controller without adaptation. The time history of the inertia parameters are shown in Fig. 8. The horizontal lines are the actual values of the parameters. As shown in Fig. 8, parameter convergence is achieved for this maneuver.

Conclusions

We have developed algorithms for controlling the spacecraft attitude in orbit while simultaneously tracking a desired power profile using a cluster of VSCMGs. For attitude tracking, both a model-based control that assumes exact knowledge of the spacecraft inertia matrix and an adaptive control that deals with the uncertainty of the inertia matrix have been proposed. These control laws have been augmented with a power-tracking algorithm, to solve for a velocity steering law for an IPACS. The scheme is similar to previous results that decompose the torque into two perpendicular spaces: one for attitude control and the other for power tracking.[6,7] Although the VSCMG system does not exhibit gimbal lock in the attitude-tracking mode, singularities may still occur if a power profile must also be followed. This problem can be solved using any of the singularity avoidance methods for a conventional CMG system. A wheel speed equalization method has also been devised to reduce the possibility of singularity and to avoid actuator saturation problems. Numerical examples based on a realistic scenario demonstrate the efficacy of the proposed control methods.

Acknowledgment

Support for this work has been provided through Air Force Office of Scientific Research Award F49620-00-1-0374.

References

[1]Roes, J. B., "An Electro-Mechanical Energy Storage System for Space Application," *Progress in Astronautics and Rocketry*, Vol. 3, Academic Press, New York, 1961, pp. 613–622.

[2]Anderson, W., and Keckler, C., "An Integrated Power/Attitude Control System (IPACS) for Space Application," *Proceedings of the 5th IFAC Symposium on Automatic Control in Space*, Pergamon, New York, 1973, pp. 81, 82.

[3]Cormack, A., III, "Three Axis Flywheel Energy and Control Systems," NASA Technical Report, TN-73-G&C-8, North American Rockwell Corp., 1973.

[4]Notti, J., Cormack, A., III, Schmill, W., and Klein, W., "Integrated Power/Attitude Control System (IPACS) Study: Volume II—Conceptual Designs," NASA Technical Report, CR-2384, Rockwell International Space Div., Downey, CA, 1974.

[5]Lange, T., "Optimal Magnetic Bearing Control for High-Speed Momentum Wheels," *Journal of Guidance, Control, and Dynamics*, Vol. 8, No. 6, 1985, pp. 737–742.

[6]Tsiotras, P., Shen, H., and Hall, C., "Satellite Attitude Control and Power Tracking with Energy/Momentum Wheels," *Journal of Guidance, Control, and Dynamics*, Vol. 24, No. 1, 2001, pp. 23–34.

[7]Hall, C. D., "High-Speed Flywheels for Integrated Energy Storage and Attitude Control," *Proceedings of the American Control Conference*, American Automatic Control Council, New York, 1997, pp. 1894–1898.

[8]Richie, D. J., Tsiotras, P., and Fausz, J. L., "Simultaneous Attitude Control and Energy Storage Using VSCMGs: Theory and Simulation," *Proceedings of the American Control Conference*, American Automatic Control Council, New York, 2001, pp. 3973–3979.

[9]Caswell, P., "Getting Flywheels Ready to Fly," GRC News Release 00-017 [on line] URL:http://www.lerc.nasa.gov/WWW/PAO/pressrel/2000/00-017.html [cited 15 Jan. 2002], NASA John H. Glenn Research Center, at Lewis Field, OH, March 2000.

[10]Schaub, H., Vadali, S. R., and Junkins, J. L., "Feedback Control Law for Variable Speed Control Moment Gyroscopes," *Journal of the Astronautical Sciences*, Vol. 46, No. 3, 1998, pp. 307–328.

[11]Ford, K. A., and Hall, C. D., "Singular Direction Avoidance Steering for Control-Moment Gyros," *Journal of Guidance, Control, and Dynamics*, Vol. 23, No. 4, 2000, pp. 648–656.

[12]Oh, H., and Vadali, S., "Feedback Control and Steering Laws for Spacecraft Using Single Gimbal Control Moment Gyro," *Journal of the Astronautical Sciences*, Vol. 39, No. 2, 1991, pp. 183–203.

[13]Schaub, H., and Junkins, J. L., "Singularity Avoidance Using Null Motion and Variable-Speed Control Moment Gyros," *Journal of Guidance, Control, and Dynamics*, Vol. 23, No. 1, 2000, pp. 11–16.

[14]Ford, K. A., and Hall, C. D., "Flexible Spacecraft Reorientations Using Gimbaled Momentum Wheels," *Advances in the Astronautical Sciences, Astrodynamics*, edited by F. Hoots, B. Kaufman, P. J. Cefola, and D. B. Spencer, Vol. 97, Univelt, San Diego, CA, 1997, pp. 1895–1914.

[15]Schaub, H., "Novel Coordinates for Nonlinear Multibody Motion with Application to Spacecraft Dynamics and Control," Ph.D. Dissertation, Aerospace Engineering Dept., Texas A&M Univ., College Station, TX, May 1998.

[16]Ahmed, J., Coppola, V., and Bernstein, D., "Adaptive Asymptotic Tracking of Spacecraft Attitude Motion with Inertia Matrix Identification," *Journal of Guidance, Control, and Dynamics*, Vol. 21, No. 5, 1998, pp. 684–691.

[17]Bishop, R., Paynter, S., and Sunkel, J., "Adaptive Control of Space Station with Control Moment Gyros," *IEEE Control Systems Magazine*, Vol. 12, No. 5, 1992, pp. 23–28.

[18]Sheen, J., and Bishop, R., "Adaptive Nonlinear Control of Spacecraft," *Proceedings of the American Control Conference*, American Automatic Control Council, New York, 1994, pp. 2867–2871.

[19]Ahmed, J., and Bernstein, D., "Adaptive Control of a Dual-Axis CMG with an Unbalanced Rotor," *Proceedings of the 37th IEEE Conference on Decision and Control*, Inst. of Electrical and Electronic Engineers, Piscataway, NJ, 1992, pp. 4531–4536.

[20]Slotine, J., and Li, W., *Applied Nonlinear Control*, Prentice–Hall, Upper Saddle River, NJ, 1991, pp. 422–433.

[21]Zaremba, A., "An Adaptive Scheme with Parameter Identification for Spacecraft Attitude Control," *Proceedings of the American Control Conference*, American Automatic Control Council, New York, 1997, pp. 552–556.

[22]Schaub, H., Akella, M. R., and Junkins, J. L., "Adaptive Realization of Linear Closed-Loop Tracking Dynamics in the Presence of Large System Model Errors," *Journal of the Astronautical Sciences*, Vol. 48, No. 4, 2000, pp. 537–551.

[23]Tsiotras, P., "Stabilization and Optimality Results for the Attitude Control Problem," *Journal of Guidance, Control, and Dynamics*, Vol. 19, No. 4, 1996, pp. 772–779.

[24]Schaub, H., and Junkins, J. L., "Stereographic Orientation Parameters for Attitude Dynamics: A Generalization of the Rodrigues Parameters," *Journal of the Astronautical Sciences*, Vol. 44, No. 1, 1996, pp. 1–19.

[25]Shuster, M. D., "A Survey of Attitude Representations," *Journal of the Astronautical Sciences*, Vol. 41, No. 4, 1993, pp. 439–517.

[26]Tsiotras, P., Junkins, J. L., and Schaub, H., "Higher Order Cayley-Transforms with Applications to Attitude Representations," *Journal of Guidance, Control, and Dynamics*, Vol. 20, No. 3, 1997, pp. 528–534.

[27]Khalil, H. K., *Nonlinear Systems*, 2nd ed., Prentice–Hall, Upper Saddle River, NJ, 1996, pp. 113–116.

[28]Margulies, G., and Aubrun, J. N., "Geometric Theory of Single-Gimbal Control Moment Gyro Systems," *Journal of the Astronautical Science*, Vol. 26, No. 2, 1978, pp. 159–191.

[29]Cornick, D. E., "Singularity Avoidance Control Laws for Single Gimbal Control Moment Gyros," *Proceedings of the AIAA Guidance and Control Conference*, AIAA, New York, 1979, pp. 20–33.

[30]Heiberg, C. J., Bailey, D., and Wie, B., "Precision Spacecraft Pointing Using Single-Gimbal Control Moment Gyroscopes with Disturbance," *Journal of Guidance, Control, and Dynamics*, Vol. 23, No. 1, 2000, pp. 77–85.

[31]Horn, R., and Johnson, C. R., *Matrix Analysis*, Cambridge Univ. Press, Cambridge, England, U.K., 1985, pp. 427, 449.

[32]Kurokawa, H., "A Geometry Study of Single Gimbal Control Moment Gyros—Singularity Problem and Steering Law," TR 175, Mechanical Engineering Lab., Tsukuba, Ibaraki, Japan, Jan. 1998.